Prognostication of Recovery Following Stroke Using the Comparison of CT and Technetium-99m HM-PAO SPECT

James M. Mountz, Jack G. Modell, Norman L. Foster, Erin S. DuPree, Robert J. Ackermann, Neil A. Petry, Laurie E. Bluemlein, and David E. Kuhl

Department of Internal Medicine, Division of Nuclear Medicine, Department of Psychiatry, Department of Neurology, University of Michigan Medical Center, Ann Arbor, Michigan

This study investigated the possibility that a relationship between the anatomic defects observed on computed tomography (CT) and the functional defects observed on single photon emission computed tomography (SPECT) might be used as an outcome measure to predict clinical recovery from the neurologic deficits induced by stroke. Twenty-seven patients with stroke location limited primarily to cerebral cortex were included in the study: each patient underwent a cranial CT scan, ^{99m}Tc hexamethylpropyleneamineoxime SPECT cerebral perfusion scan, and an initial and 1-yr follow-up neurologic examination. A strongly positive correlation between the ratio of the SPECT to CT volume defect sizes (SPECT ÷ CT) and recovery following stroke was found, such that the greater the SPECT to CT ratio, the better the subsequent recovery of neurological deficits. Discriminant function analysis revealed that the best predictor of clinical outcome following stroke was the log-transformation of SPECT ÷ CT. The results suggest that the relationship between the perfusion defects and tissue loss measured by SPECT and CT imaging may have prognostic utility following stroke limited primarily to cerebral cortex.

J Nucl Med 1990; 31:61–66

Stroke is the third most common cause of death in North America, afflicting nearly 500,000 new victims a year, and having an overall prevalence of nearly two million men and women (*1*). Accurate diagnosis and determination of prognosis following stroke are critical to proper patient management (*2–4*). Stroke diagnosis traditionally has been confirmed by anatomic imaging techniques such as computed tomography (CT) (*5,6*) and more recently, by magnetic resonance imaging (MRI) (*7,8*). The early detection and diagnosis of stroke has been further aided by functional imaging using single photon emission computed tomography (SPECT) (*9–15*) and positron emission tomography (PET) (*16–20*).

Despite literature which supports the use of radionuclide imaging techniques in the detection and diagnosis of stroke (*21–23*), objective criteria for prognostication of clinical recovery from the neurologic deficits following stroke have not been established (*24–28*). In an effort to address this need, we undertook a study to seek a relationship between the anatomic defects observed on CT and the functional defects observed on SPECT which might be used as an outcome measure to predict clinical recovery (recovery prognosis) from the neurologic deficits induced by the stroke.

MATERIALS AND METHODS

The study population consisted of 27 patients (age 26–85 yr; six females, 21 males) with a history of solitary stroke which was primarily limited to the cerebral cortex (Table 1); average subjacent white matter involvement was <10% of the measured CT volume defect. The interval between the symptom(s) referent to the ictal event under study and initial evaluation ranged between 0.1 and 66 m. This study was approved by the Human Use Committee of the University of Michigan Medical Center, and informed consent was obtained from all subjects.

Patients were evaluated by CT, SPECT, and a complete neurologic examination by a Broad-certified neurologist (N.L.F.). All patients received these examinations within a 3-day time span in order to assure comparable results between CT, SPECT, and the neurologic examination. Severity of stroke and localization of the lesion by clinical symptoms were assessed in the neurologic exam. Severity of stroke was rated as *mild* if there were focal neurologic deficits on exam that did not result in functional impairment (e.g., asymmetric deep tendon reflexes in the absence of gross motor deficits), *moderate* if the deficits produced limited functional impairment, or *severe* if there was hemiplegia or significant change in level of consciousness. At the time of the one year follow-up evaluation, the degree of recovery from the initial stroke-induced symptoms was classified as: no recovery, some recovery (improvement, but still functionally impaired), near-complete recovery (minimal residual neurologic deficits and functional

Received Apr. 3, 1989; revision accepted Aug. 2, 1989.

For reprints contact: James M. Mountz, MD, PhD, University of Michigan Medical Center, Div. of Nuclear Medicine, 1500 East Medical Center Dr., Ann Arbor, MI 48109-0028.

TABLE 1
Study Population Characteristics*

	Sex/age	Interval since stroke (mo)	Severity of stroke	Location	Recovery classification	CT lesion size (cm^3)	SPECT lesion size (cm^3)	Log (SPECT + CT)
1	M/62	6	Severe	L hemisphere	None	76	70	−0.04
2	M/66	11	Severe	L hemisphere	None	161	170	0.02
3	M/78	6	Mild	R hemisphere	None	3.7	4.3	0.06
4	M/64	7	Moderate	R hemisphere	None	98	109	0.05
5	M/58	2	Moderate	R anterior	None	24	33	0.14
6	M/65	2	Moderate	R posterior	None	3.4	3.5	0.01
7	F/75	0.2	Mild	L posterior	None	0.4	0.45	0.04
8	M/70	65	Mild	L anterior	None	3.6	4.6	0.11
9	M/64	4	Severe	R hemisphere	Some	42	37	−0.06
10	M/55	12	Moderate	R posterior	Some	2.2	2.2	0
11	M/64	4	Severe	L middle	Some	75	72	−0.02
12	M/55	12	Moderate	L posterior	Some	5.5	5.6	0.01
13	F/72	5	Severe	R middle	Some	2.7	2.9	0.03
14	M/55	12	Moderate	R posterior	Some	10	9.9	−0.01
15	M/57	3	Severe	L middle	Near-cmpl	6.1	23	0.58
16	M/85	3	Severe	L hemisphere	Near-cmpl	9.2	47	0.71
17	F/63	0.5	Moderate	L middle	Near-cmpl	0.03	13	2.6
18	M/66	64	Severe	R anterior	Near-cmpl	0.1	3.4	1.6
19	F/26	0.1	Moderate	L middle	Near-cmpl	2.5	24	0.97
20	M/66	0.7	Severe	L middle	Near-cmpl	0.02	10	2.7
21	F/43	0.1	Moderate	L middle	Near-cmpl	1.4	2.7	0.30
22	M/66	3	Mild	R hemisphere	Near-cmpl	0.01	0.14	1.1
23	M/65	2	Moderate	L anterior	Near-cmpl	9.9	34	0.54
24	M/65	8	Mild	L anterior	Near-cmpl	4.8	12	0.40
25	M/73	0.2	Moderate	L middle	Near-cmpl	0.8	6.4	0.88
26	F/80	7	Mild	R middle	Complete	0.5	1.7	0.58
27	M/65	66	Mild	L middle	Complete	4.0	6.9	0.24

* Sex/age, interval since stroke, initial severity of stroke, stroke location (divided into anterior, middle, or posterior sectors), recovery classification (near-cmpl = near-complete), stroke size (CT), stroke size (SPECT), and $\log_{10}$ (SPECT + CT).

impairment), or complete recovery. No patient had a second symptomatic neurologic event during the period of study. The same neurologist performed both the initial and one-year follow-up evaluations to ensure consistency in stroke recovery classification; this neurologist was blind to the SPECT and CT data.

SPECT imaging was performed using a rotating GE 400 AC gamma camera equipped with a general, all-purpose, low-energy, parallel hole collimator. SPECT acquisition parameters were: 360° rotation, 64 stops, and 30 sec per stop; yielding between 5 and 8 million total counts per image (*29*). The radiopharmaceutical technetium-99m hexamethyl-propyleneamineoxime ([^{99m}Tc]HM-PAO) (*30,31*) was utilized for SPECT imaging; this tracer was supplied in single dose vials by the Amersham Corporation. Each vial was reconstituted with 25–30 mCi [^{99m}Tc]sodium pertechnetate in 5 ml saline eluted from a commercially available ^{99m}Mo/^{99m}Tc generator. The prepared tracer had radionuclidic purity greater than 99%, and <2% free or reduced-hydrolyzed ^{99m}Tc-sodium-pertechnetate; the chromatographic quality control assay demonstrated that in all cases the tracer had greater than 95% lipophilicity. Imaging commenced five minutes after i.v. administration of ~20 mCi of [^{99m}Tc]HM-PAO into an antecubital vein. All patients were injected within 30 min of vial reconstitution. Image data were processed on the Siemens MicroDelta computer using a Butterworth filter, frequency cutoff of 0.5 Nyquist order 5.0, and attenuation corrected using the Chang method (*32*). Image acquisition and reconstruction were performed simultaneously. Sagittal (y-axis) 3-slice averaging was performed using a 9-point smooth. No transverse (x-axis) averaging or smoothing were performed. The image matrix size was 64 × 64 pixels. An average of 20 SPECT image planes, 0.625 cm thick, were required to image the entire brain. SPECT pixel size was 0.625 cm in all three dimensions. CT scans were performed on the GE 9800 scanner, and contiguous 10-mm-thick sections (~13 slices) were obtained through the entire cranial vault.

SPECT image analysis was performed by drawing regions of interest around the entire lesion in the involved hemisphere, and around any involved, immediately subjacent brain tissue. The lesion margin was defined where tracer uptake values (counts/pixel) around the lesion increased to within 10% of those in the contralateral region of the uninvolved hemisphere as determined by moving a horizontal profile through the portion of brain containing the lesion. The circumscribed region containing the lesion was then mirrored on every slice containing a visible defect to the corresponding zone in the uninvolved hemisphere by direct translation of the region coordinates across the longitudinal axis. Patients with blood flow defects that crossed the midline (longitudinal axis) were

excluded from analysis. In this fashion, a SPECT volume defect in cubic centimeters was determined using the equation (*33*):

$$V_T = V_P \times \sum_{i=1}^{n} \left[\frac{M_i - S_i}{M_i}\right] \times P_i \ , \qquad (1)$$

where V_T is the total volume (cc) defect of the lesion, V_p is the volume (cc) of the individual pixel, S_i represents the single photon emission counts within the circumscribed region of stroke, M_i represents the single photon emission counts within the mirrored region in the uninvolved hemisphere, and P_i is the number of pixels in the region of interest; the sum of i is taken over all scan planes that show a diminution of tracer uptake in the hemisphere containing the stroke. In this manner a SPECT defect-volume equivalent to a hypothetical volume of zero perfusion is obtained which can then be appropriately compared to the CT lesion defect-volume. The CT defect-volume (cc) was defined as the total volume of infarcted tissue visible on the CT scans as determined by circumscribing all visible areas of low attenuation in each involved plane and then summing the single-plane defect volumes. In each case, the zone of low attenuation was clearly visible and sharply demarcated from normal-appearing brain, and the lesion perimeter was drawn from visual inspection of each CT slice.

Data Analysis

Data analysis was conducted with the goal of testing the possibility that the relationship between the anatomic volume defect size observed on CT and the functional defect size calculated from the SPECT scan might be used as an outcome measure to predict clinical recovery from the deficits induced by the stroke under study. Also tested were possible confounding contributions from significant associations between other independent variables; these included subject sex and age, time-interval between the symptom(s) referent to the ictal event under study and the SPECT scan, stroke location, and the CT and SPECT stroke defect sizes. Degree of recovery at 1-yr follow-up served as the dependent variable; for the purpose of providing a sufficient and balanced number of subjects in each recovery group, this category was divided into those subjects who experienced either: (a) no recovery or some recovery (n = 14) or (b) near-complete or complete recovery (n = 13) from the stroke-induced neurologic deficits.

A stepwise discriminant analysis ($\alpha = 0.05$) was performed to assess the contribution of each of the independent variables–separately and in combination–to the dependent outcome measure (*34*). Also analyzed were the ratio between the SPECT to CT volume size (SPECT ÷ CT) and the $\log_{10}$ transformation of SPECT ÷ CT. Logarithms were introduced since they provided a more normal statistical distribution of the quotients obtained (SPECT ÷ CT), especially when dividing by small CT sizes. Additionally, chi-squared-contingency, and linear-correlational analyses ($\alpha = 0.05$) were performed on the independent variables to test for the existence of significant associations among them.

RESULTS

The experimental data for all patients are shown in Table 1. Discriminant analysis for each of the independent variables revealed that only the logarithm of the SPECT to CT lesion volume ratio [log(SPECT ÷ CT)] and logarithm of the CT lesion volume [logCT] had significant effects—considered separately—on the degree of recovery (for log(SPECT ÷ CT), positive correlation, $F_{1,25} = 20.64$, $p < 0.001$); for logCT, inverse correlation, $F_{1,25} = 12.32$, $p < 0.005$). However, when log (SPECT ÷ CT) is entered into the analysis as the first independent variable, the partial correlations of all other independent experimental measures become nonsignificant ($F_{1,25} = 20.64$, $p < 0.001$ for log (SPECT ÷ CT); $F_{1,24} = 0.40$, $p \sim 0.5$ for log CT). Forcing logCT into the first step of the analysis does not similarly eliminate log(SPECT ÷ CT) as a significant variable ($F_{1,24} = 5.8$, $p < 0.05$). These data are summarized in a frequency analysis of recovery versus log (SPECT ÷ CT) (Fig. 1), which shows a clear separation of the two clinical outcome groups by the log (SPECT ÷ CT).

Calculated discriminant function classification equations are:

$$-0.0919 \times \log(\text{SPECT}\div\text{CT}) - 0.694 \qquad (2)$$

for the group showing poorer clinical outcome; and,

$$3.19 \times \log(\text{SPECT}\div\text{CT}) - 2.32 \qquad (3)$$

for the group showing near-complete to complete recovery.

Simplified, for eq. 3 minus eq. 2, or

$$3.28 \times \log(\text{SPECT}\div\text{CT}) - 1.63 > 0 \qquad (4a)$$

predicted outcome is near-complete to complete recovery, and for

$$3.28 \times \log(\text{SPECT}\div\text{CT}) - 1.63 < 0 \qquad (4b)$$

predicted outcome is in the poorer prognostic category.

Application of these equations to the data accurately classified 100% (14 out of 14) of those patients with the poorer outcomes, and 70% (9 out of 13) of those with near-complete to complete recoveries. The contingency and correlational analyses showed no significant associations among the independent measures (stroke size, interval between ictus and evaluation in the study,

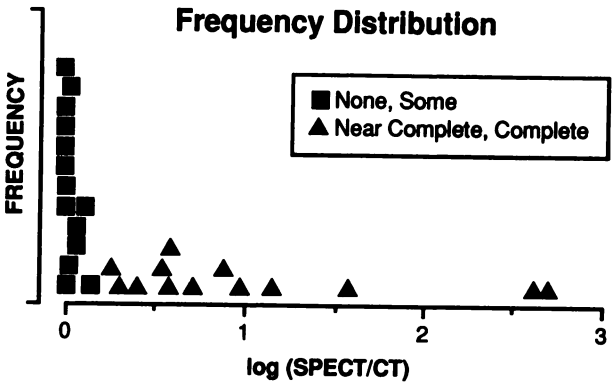

FIGURE 1
Frequency distribution of the log (SPECT ÷ CT) volume defects demonstrating the ability of this function to separate patients with good prognosis from those with poor prognosis.

location of stroke, clinical severity of stroke) except for a reciprocal correlation between logCT and log (SPECT ÷ CT) ($r^2 = 0.56$; $F_{1,25} = 34.8$, $p < .001$).

An alternative view of the data can be seen in Figure 2, which shows the linear regression plots of the absolute values of the CT volume defect versus SPECT volume defect for each of the two clinical outcome groups. It can be seen that for the group with the poorer clinical outcome (Fig. 2A), the slope of the regression line (i.e. SPECT ÷ CT) is near unity; for the group having near-complete or complete recovery (Fig. 2B), the slope is 3.4, indicating SPECT lesion volumes are considerably larger than the corresponding CT lesion volumes.

Figure 3 illustrates a typical CT and SPECT scan lesion analyzed. The patient is a 58-yr-old male with a history of chronic stroke involving the right frontal region (Table 1, Patient 5). The patient presented with moderate left lower-extremity impairment; he had no recovery of the neurologic deficit during the year of follow-up.

DISCUSSION

This study sought potential correlations between the anatomic volume defects observed on the CT image and the blood flow defects observed on the SPECT image; and clinical recovery from the neurological deficits induced by the stroke under study. The study was limited to patients with primarily cortical strokes involving only one cerebral hemisphere. Using quantitative methods to determine the stroke-induced SPECT and CT volume size, we found a strongly positive correlation between the log (SPECT ÷ CT) and recovery, and the absence of significant correlations between recovery and the other independent variables assessed.

Prior work has indicated that the SPECT volume defect in stroke generally appears larger than that of the corresponding CT defect (*35–37*). The findings of this study are of particular significance because they demonstrate that by using quantitative methods which avoid the use of subjective visual impressions (*33*) to determine SPECT defect-volumes, the SPECT and CT volume defects may not only be nearly equal in many cases, but such cases may have a relatively poor prognosis. These findings suggest that high SPECT to CT volume defect ratios indicate the presence of viable—though dysfunctional—tissue which retains the capacity for restoration of more normal function, possibly due to subsequent improvement in blood flow to this tissue. On the other hand, where SPECT to CT volume defects are nearly equal, no such capacity for restoration of lost function exists.

Discriminant function analysis revealed that the larger the value of log (SPECT ÷ CT), the greater the likelihood of a good clinical outcome. In this study, all patients with log (SPECT ÷ CT) < 0.2 or [SPECT ÷ CT < ~1.5] fell into the poorer outcome category, and all with log (SPECT ÷ CT) > 0.2 or [SPECT ÷ CT > ~1.5] had good recoveries. The discriminant function equations, based on the distribution of the obtained imaging data, yielded an overall correct classification of outcome based on log (SPECT ÷ CT) alone in 85% of cases.

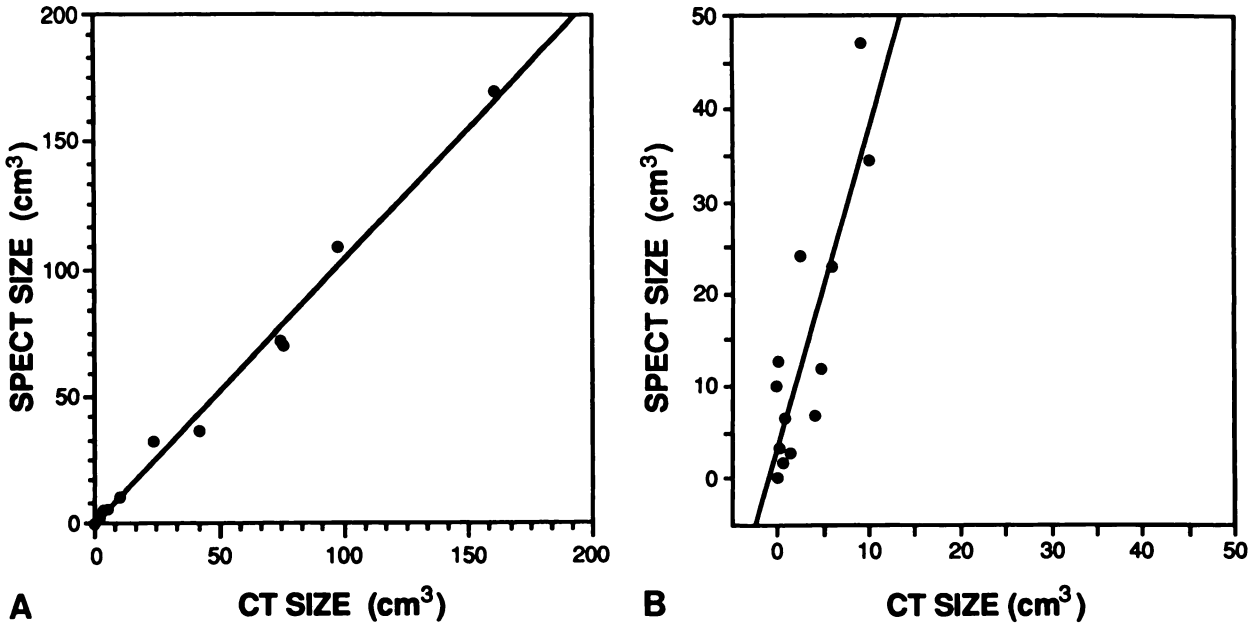

FIGURE 2

A: Linear regression plots of the CT volume defect versus SPECT volume defect for the group with the poorer clinical outcome (SPECT = −0.5 + 1.05 × CT; n = 14, $r^2 = 0.98$, $p < 0.01$). B: Linear regression plots of the CT volume defect versus SPECT volume defect for the group with near complete to complete recovery (SPECT = 3.7 + 3.4 × CT; n = 13, $r^2 = 0.74$, $p < 0.01$).

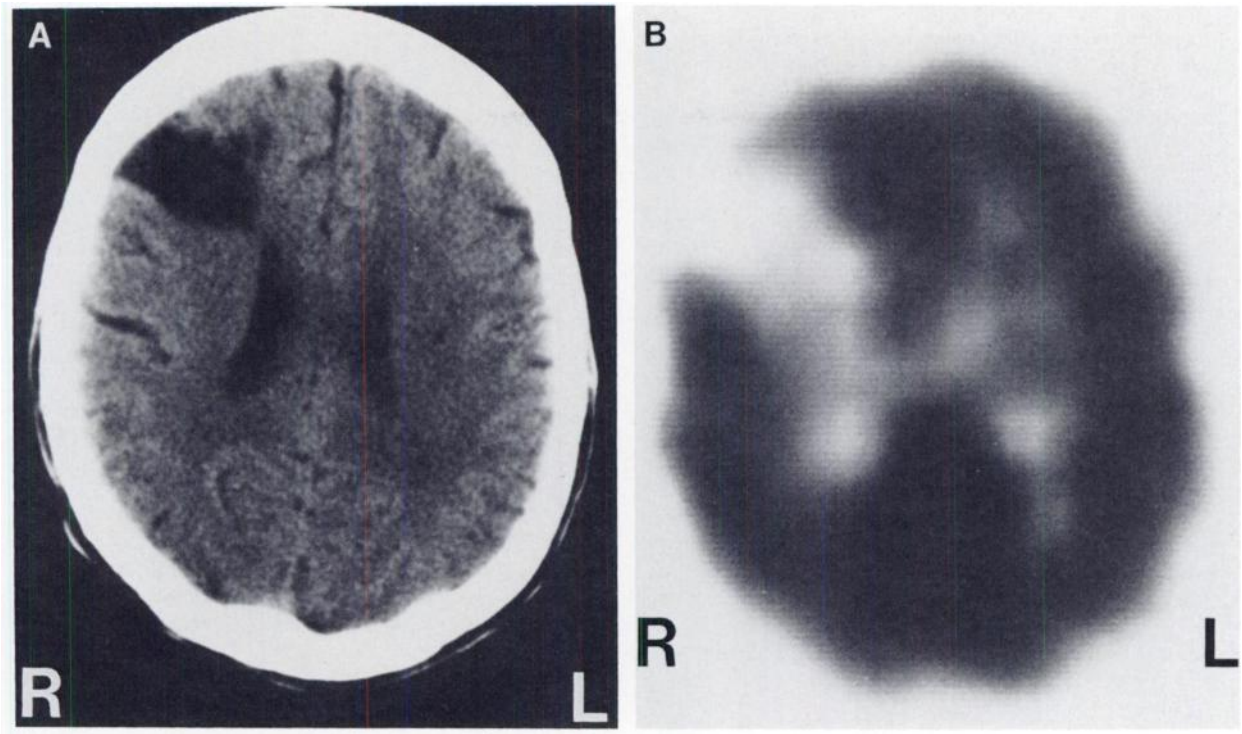

FIGURE 3
A: Representative stroke lesion in a 58-yr-old male with a chronic right anterior cortical infarction (Table 1, Patient 5). B: SPECT scan slice through the center of the lesion shown in Figure 3A.

Though the inverse correlation between logCT and degree of recovery may influence the results (i.e., larger lesions causing poorer prognosis), the discriminant analysis clearly revealed that log (SPECT ÷ CT) was superior to logCT size (alone or in combination) in accounting for a highly significant portion of the outcome variance. Further supporting the superiority of log (SPECT ÷ CT) to logCT size alone, when the five largest lesions are excluded from the analysis, the positive association between log (SPECT ÷ CT) and prognosis is preserved ($F_{1,20} = 12.7$, $p < 0.01$), but the significant relationship between CT size and prognosis disappears ($F_{1,20} = 0.40$, $p \sim 0.5$).

The inherent limitations and difficulties in stroke classification on clinical grounds are well-documented (*1,38,39*), and may have introduced some uncontrolled variance (subjectively) into our findings. That a strong correlation between log (SPECT ÷ CT) and prognosis was found, nonetheless, is particularly noteworthy and suggests that this correlation may be sufficiently robust to allow application of these methods in clinical settings. Application of equations 4a and 4b in these settings may provide a very useful mathematical method to assess stroke recovery prognosis in gray-matter stroke from the relationship between the functional SPECT, and the anatomic CT images alone. A prospective study to more completely characterize these relationships should, however, be carried out. It is suggested that these methods may also be applicable to other neurologic disorders in which a similar discrepancy exists between anatomic, and functional tissue defect size.

ACKNOWLEDGMENT

The authors thank Stephen Schmaltz, MPH, University of Michigan Clinical Research Center, for providing statistical consultation and data analysis. They also thank Ms. Merribeth Adams for her assistance in this work and extend their appreciation to the Amersham Corporation for providing the radiopharmaceutical.

REFERENCES

1. Hachinski V, Norris JW. The problem. In: Plum F, ed. *The acute stroke.* Philadelphia: F.A. Davis Co; 1985:1–12.
2. Friedman SG, Lamparello PJ, Riles TS, Imparato AM. Revascularization of the external carotid artery. *Arch Surg* 1988; 123:497–499.
3. Pritz MB. Carotid endarterectomy after recent stroke: preliminary observations in patients undergoing early operation. *Neurosurgery* 1986; 19:604–609.
4. Zivin JA, Lyden PD, DeGirolami U, et al. Tissue plasminogen activator: reduction of neurologic damage after experimental embolic stroke. *Arch Neurol* 1988; 45:387–391.
5. Wang AM, Lin JCT, Rumbaugh CL. What is expected of CT in the evaluation of stroke? *Neuroradiology* 1988; 30:54–58.
6. Meyer JS, Okayasu H, Tachibana H, Okabe T. Stable xenon CT CBF measurements in prevalent cerebrovascular disorders

(stroke). *Stroke* 1984; 15:80–90.
7. Unger EC, Gado MH, Fulling KF, Littlefield JL. Acute cerebral infarction in monkeys: an experimental study using MR imaging. *Radiology* 1987; 162:789–795.
8. Brant-Zawadzki M, Weinstein P, Bartkowski H, Moseley M. MR imaging and spectroscopy in clinical and experimental cerebral ischemia: a review. *Am J Roentgenol* 1987; 148:579–588.
9. Kuhl DE, Edwards RQ. Image separation radioisotope scanning. *Radiology* 1963; 80:653–662.
10. Ell PJ, Hocknell JML, Jarritt PH, et al. A ^{99m}Tc-labelled radiotracer for the investigation of cerebral vascular disease. *Nucl Med Commun* 1985; 6:437–441.
11. Ell PJ, Lui D, Cullum I, Jarritt PH, Donaghy M, Harrison MJG. Cerebral blood flow studies with ^{123}iodine-labelled amines. *Lancet* 1983; ii:1348–1352.
12. Holman BL, Hill TC, Polak JF, Lee RGL, Royal HD, O'Leary DH. Cerebral perfusion imaging with iodine 123-labeled amines. *Arch Neurol* 1984; 41:1060–1063.
13. Kuhl DE, Barrio JR, Huang S, et al. Quantifying local cerebral blood flow by N-isopropyl-p-[^{123}I]iodoamphetamine (IMP) tomography. *J Nucl Med* 1982; 23:196–203.
14. Brott TG, Gelfand MJ, Williams CC, Spilker JA, Hertzberg VS. Frequency and patterns of abnormality detected by iodine-123 amine emission CT after cerebral infarction. *Radiology* 1986; 158:729–734.
15. Creutzig H, Schober O, Gielow P, et al. Cerebral dynamics of N-Isopropyl-(^{123}I))p-iodoamphetamine. *J Nucl Med* 1986; 27:178–183.
16. Ter-Pogossian MM, Phelps ME, Hoffman EJ, Mullani NA. A positron-emission transaxial tomograph for nuclear imaging (PETT). *Radiology* 1975; 114:89–98.
17. Heiss WD, Herholz K, Böcher-Schwarz HG, et al. PET, CT, and MR imaging in cerebrovascular disease. *J Comput Assist Tomogr* 1986; 10:903–911.
18. Hakim AM, Pokrupa RP, Villanueva J, et al. The effect of spontaneous reperfusion on metabolic function in early human cerebral infarcts. *Ann Neurol* 1987; 21:279–289.
19. Ackerman RH, Alpert NM, Correia JA, et al. Positron imaging in ischemic stroke disease. *Ann Neurol* 1984; 15(suppl):S126–S130.
20. Levine RL. The study of cerebral ischemic reversibility: Part 1. A review of positron imaging studies. *Am J Physiol Imag* 1986; 1:54–58.
21. Royal HD, Hill TC, Holman BL. Clinical brain imaging with isopropyl-iodoamphetamine and SPECT. *Semin Nucl Med* 1985; 15:357–376.
22. Raynaud C, Rancurel G, Samson Y, et al. Pathophysiologic study of chronic infarcts with I-123 isopropyl iodo-amphetamine (IMP): the importance of periinfarct area. *Stroke* 1987; 18:21–29.
23. Spreafico G, Cammelli F, Gadola G, et al. Initial experience with SPECT of the brain using ^{99m}Tc-hexamethyl-propyleneamine oxime (^{99m}Tc-HM-PAO). *Eur J Nucl Med* 1987; 12:557–559.
24. Merrick NJ, Brook RH, Fink A, Solomon DH. Use of carotid endarterectomy in five California Veterans Administration medical centers. *JAMA* 1986; 256:2531–2535.
25. Awad IA, Spetzler RF. Extracranial-intracranial bypass surgery: A critical analysis in light of the international cooperative study. *Neurosurgery* 1986; 19:655–664.
26. Haynes RB, Mukherjee J, Sackett DL, et al. Functional status changes following medical or surgical treatment for cerebral ischemia. *JAMA* 1987; 257:2043–2046.
27. Foulkes MA, Wolf PA, Price TR, Mohr JP, Hier DB. The stroke data bank: Design, methods, and baseline characteristics. *Stroke* 1988; 19:547–554.
28. König B, Donis J, Mostbeck A, Köhn H. Die single-photon emissionstomographie (SPECT) mit ^{123}I-amphetamin bei zerebralen ischämischen durchblutungsstörungen. *Nuklearmedizin* 1987; 26:45–51.
29. Keyes JW Jr. Perspectives on tomography. *J Nucl Med* 1982; 23:633–640.
30. Neirinckx RD, Canning LR, Piper IM, et al. Technetium-99m d,l-HM-PAO: A new radiopharmaceutical for SPECT imaging of regional cerebral blood perfusion. *J Nucl Med* 1987; 28:191–202.
31. Podreka I, Suess E, Goldenberg G, et al. Initial experience with technetium-99m HM-PAO brain SPECT. *J Nucl Med* 1987; 28:1657–1666.
32. Chang L. A method for attenuation correction in radionuclide computed tomography. *IEEE Trans Nucl Sci* 1978; NS-25:638–643.
33. Mountz JM. A method of analysis of SPECT blood flow image data for comparison with computed tomography. *Clin Nucl Med* 1989; 14:192–196.
34. Morrison DF. Multivariant statistical methods. New York: McGraw Hill, 1976:239–246.
35. Lee RGL, Hill TC, Holman BL, Royal HD, O'Leary DH, Clouse ME. Predictive value of perfusion defect size using N-isopropyl-(I-123)-p-iodoamphetamine emission tomography in acute stroke. *J Neurosurg* 1984; 61:449–452.
36. Hill TC, Magistretti PL, Holman BL, et al. Assessment of regional cerebral blood flow (rCBF) in stroke using SPECT and N-isopropyl-(I-123)-p-iodoamphetamine (IMP). *Stroke* 1984; 15:40–45.
37. Higa T, Tanaka T, Ikekubo K, Komatsu T, Torizuka K. SPECT with N-isopropyl-p iodoamphetamine in occlusive cerebrovascular diseases. *Clin Nucl Med* 1986; 12:855–859.
38. Norris JW. Comment on "study design of stroke treatment." *Stroke* 1982; 13:257–258.
39. Cote R, Battista RN, Wolfson C, Boucher J, Adam J, Hachinski V. Validity and reliability of the Canadian neurological scale. *J Cereb Blood Flow Metab* 1989; 9:s595.